Diagnosis of a low pressure capacitively coupled argon plasma by using a simple collisional-radiative model*

Yu Yi-Qing(虞一青), Xin Yu(辛 煜)†, and Ning Zhao-Yuan(宁兆元)‡

Jiangsu Key Laboratory of Thin Films, School of Physical Science and Technology, Soochow University, Suzhou 215006, *China*

(Received 7 April 2010; revised manuscript received 2 August 2010)

This paper proposes a simple collisional-radiative model to characterise capacitively coupled argon plasmas driven by conventional radio frequency in combination with optical emission spectroscopy and Langmuir probe measurements. Two major processes are considered in this model, electron-impact excitation and the spontaneous radiative decay. The diffusion loss term, which is found to be important for the two metastable states ($4s[3/2]_2$, $4s'[1/2]_0$), is also taken into account. Behaviours of representative metastable and radiative states are discussed. Two emission lines (located at 696.5 nm and 750.4 nm) are selected and intensities are measured to obtain populated densities of the corresponding radiative states in the argon plasma. The calculated results agree well with that measured by Langmuir probe, indicating that the current model combined with optical emission spectroscopy is a candidate tool for electron density and temperature measurement in radio frequency capacitively coupled discharges.

Keywords: capacitively coupled plasma, collisional-radiative model, optical emission spectroscopy, Langmuir probe

PACS: 52.80.Pi, 52.70.Kz, 52.25.Os **DOI:** 10.1088/1674-1056/20/1/015207

1. Introduction

Low pressure plasma discharges play an important role in materials processing, such as thin film deposition and photoresist ashing in microelectronic engineering.[1] There are several kinds of low temperature plasma sources, such as electron cyclotron resonance plasma, inductively coupled plasma and capacitively coupled plasma (CCP), etc.[2−5] Among them, the CCP is an important tool for dielectric etching with high fidelity due to an independent control of ion flux and energy.[6,7] Additionally, CCP can also be used in film deposition with high speed due to its high density driven by a higher frequency than conventional 13.56 MHz.[8,9]

In low pressure radio frequency (RF) discharges the energetic electrons interact with parent gas to support processes of excitation, dissociation and ionisation. Therefore, the electron temperature and density in these plasmas are two key parameters for the characterisation of low temperature plasmas. Among kinds of plasma diagnostic tools, the Langmuir probe is widely used for the characterisation of electron behaviour.[10] However, the distortions of the probe current–voltage (I–V) characteristics arisen from strong RF perturbations often occur and may influence the measurement accuracies.[11] Although there were some reports about single probe usage in CCP discharges,[12,13] the RF perturbation, such as fundamental frequency and its harmonics especially induced from relative low frequency or dual frequency, is still a serious problem.

Different from the probe method, optical emission spectroscopy (OES) is another usual tool widely used in low pressure plasma diagnostics due to its simplicity, affordability and noninvasiveness. By adding a small amount of rare gases (i.e., He, Ne, Ar, Kr and Xe) Donnelly and co-workers developed the trace rare gases OES technique[14] and applied it to the chlorine inductively coupled plasmas[15] and oxygen surface wave plasmas.[16] Palmero *et al.*[17] developed a simple collisional-radiative (CR) model for a magnetron sputtering argon plasma, which included 12 effective energy levels, and studied extensively the behaviours of the excited states. Zhu and Pu proposed a model of low pressure argon discharges. They selected two proper emission lines and successfully provided measurements of the electron density in an inductively coupled plasma by using the so-called line ratio method.[18]

In this article we present a simplified CR model contained 22 effective energy levels and apply it to

*Project supported by the National Natural Science Foundation of China (Grant Nos. 10635010 and 10775103).

†Corresponding author. E-mail: xylzf_1999@suda.edu.cn

‡E-mail: zyning@suda.edu.cn

© 2011 Chinese Physical Society and IOP Publishing Ltd

the diagnosis of low pressure argon CCP discharges driven by conventional 13.56 MHz together with OES. The electron density and temperature measured from the OES method are also compared with that of the Langmuir probe so as to confirm the validity of the CR model.

2. Argon CR model

An argon CR model contained 65 effective energy levels was proposed by Vlcek[19] and later some modifications have been made by Bogaerts *et al.*[20] and Bultel *et al.*[21] The processes considered in these models are electron impact collisions, neutral argon impact collisions, spontaneous radiative decay, etc. These models have been used to describe the argon discharges successfully from low pressure to atmospheric pressure range.[17,22–25]

Our proposed model contains 22 real and lumped levels ranging from the ground state to about 15 eV. In fact, the concentrations of those higher energy levels are relatively low in typical low pressure CCP discharges with electron temperature and density in the range of 1–7 eV and 10^9–10^{11} cm^{-3}. Yanguas *et al.*[23] have applied a CR model contained 30 effective levels (neglecting those levels above 15 eV) to a low pressure microwave discharge and in Palmero's model the highest energy level is just about 14 eV.[17]

The energy levels used in our model are listed in Table 1. The core angular momentum j_c may equal 1/2 or 3/2.[26] For a lumped energy level, its effective energy is obtained by averaging real levels and weighted by their degeneracies.

Table 1. Energy levels considered in the present argon CR model.

level number	energy/eV	degeneracy g	j_c	designation $nl[K]_J$
1	0	1	1.5	$3p^6$
2	11.548	5	1.5	$4s[3/2]_2$
3	11.624	3	1.5	$4s[3/2]_1$
4	11.723	1	0.5	$4s'[1/2]_0$
5	11.828	3	0.5	$4s'[1/2]_1$
6	12.907	3	1.5	$4p[1/2]_1$
7	13.116	20	1.5	$4p[3/2]_{1,2}$, $4p[5/2]_{2,3}$
8	13.273	1	1.5	$4p[1/2]_0$
9	13.295	8	0.5	$4p'[3/2]_{1,2}$
10	13.328	3	0.5	$4p'[1/2]_1$
11	13.480	1	0.5	$4p'[1/2]_0$
12	13.884	9	1.5	$3d[1/2]_{0,1}$, $3d[3/2]_2$
13	13.994	16	1.5	$3d[7/2]_{3,4}$
14	14.090	23	1.5	$3d[3/2]_1$, $3d[5/2]_{2,3}$, 5s
15	14.229	17	0.5	$3d'[3/2]_2$, $3d'[5/2]_{2,3}$
16	14.252	4	0.5	5s′
17	14.304	3	0.5	$3d'[3/2]_1$
18	14.509	24	1.5	5p
19	14.690	12	0.5	5p′
20	14.792	48	1.5	4d, 6s
21	14.906	56	1.5	4f
22	14.976	24	0.5	4d′, 6s′

Electron collisions play an important role in low pressure plasma discharges and in this article the electron energy distribution function (EEDF) is assumed to be Maxwellian. The electron energy distribution may deviate from Maxwellian in the low pressure discharges and affects the calculation of rate coefficients for electron impact excitation processes from the ground state (usually with threshold energy larger than 10 eV). However, as mentioned by Zhu and Pu, it is believed that the deviation from the Maxwellian distribution can be tolerable since the excitation energies of the main radiative states are close to each other.[18]

Results in Ref. [17] also show that the Maxwellian electron distribution is a reasonable assumption.

The main electron collisional processes considered are electron impact excitation/deexcitation and ionisation. The electron impact excitation/deexcitation between each two states in Table 1 are considered in our model. An electron impact excitation from a lower energy level i to another higher level j could be characterised by rate coefficient k_{ij} which could be expressed as

$$k_{ij} = \sqrt{\frac{2}{m}} \int_{E_{ij}}^{\infty} \sigma_{ij}(E) E F(E) \mathrm{d}E, \tag{1}$$

where m is the electron mass, σ_{ij} is the electron impact cross section for the transition depended on the electron kinetic energy E. The $E_{ij} = E_j - E_i$ ($E_j > E_i$) is the impact threshold energy for the transition and $F(E)$ is the electron energy probability function which is related to EEDF $f(E)$ by $f(E) = E^{1/2}F(E)$ and could be normalised as $\int_0^{\infty} \sqrt{E} F(E) \mathrm{d}E = 1$. For the inverse process, the electron impact deexcitation from level j to level i, the rate coefficient k_{ji} could be expressed by applying the detailed balance principle[23]

$$k_{ji} = \frac{g_i}{g_j} \sqrt{\frac{2}{m}} \int_{E_{ij}}^{\infty} \sigma_{ij}(E) E F(E - E_{ij}) \mathrm{d}E, \tag{2}$$

where g_i and g_j are degeneracies of level i and j, respectively.

In the past decades, some theoretical and experimental works of electron-collision cross sections have been carried out.[19,27–30] Recently the Lin's group gave some new experimental results of electron impact from the ground and metastable states to higher excited levels by using optical method.[31,32] Yanguas *et al.*[33] also gave an update of argon inelastic cross sections for plasma discharge. In this paper the analytical expressions of cross sections are based on the above-mentioned works. The cross section for electron impact excitation from level i to j is summarised as optically allowed, parity-forbidden and spin-forbidden transition, respectively.[20] For transitions between the first four 4s excited levels we used[20,23]

$$\begin{aligned} \sigma(i,j,E) = {} & 5.797 \times 10^{-15} \times \frac{g_j}{g_i} \frac{E - E_{ij}}{E} \\ & \times Q_{ij} \left(E - E_{ij}\right)^{-0.54} / \mathrm{cm}^2, \end{aligned} \tag{3}$$

where $Q_{23} = 0.2$, $Q_{24} = Q_{25} = Q_{34} = Q_{35} = 0.1$, and $\sigma(i,j,E) = 8.111 \times 10^{-16} \times \frac{g_j}{g_i} \frac{E - E_{ij}}{E} \left(E - E_{ij}\right)^{-1.04} / \mathrm{cm}^2$ for $i = 4$, $j = 5$.

The formula describing electron impact ionisation process has a similar form to that of electron impact excitation process

$$k_{i-\mathrm{ion}} = \sqrt{\frac{2}{m}} \int_{E_{i-\mathrm{ion}}}^{\infty} \sigma_{i-\mathrm{ion}}(E) E F(E) \mathrm{d}E, \tag{4}$$

where $E_{i-\mathrm{ion}}$ is the electron impact ionisation energy for level i.

The electron impact ionisation cross sections of different effective levels could be calculated[20] from

$$\begin{aligned} \sigma^{\mathrm{e}}_{i-\mathrm{ion}}(E) = {} & 4\pi a_0^2 \left(\frac{E^{\mathrm{H}}_{\mathrm{ion}}}{E_{i-\mathrm{ion}}}\right)^2 \xi_i \alpha_{i-\mathrm{ion}} \\ & \times \frac{E/E_{i-\mathrm{ion}} - 1}{\left(E/E_{i-\mathrm{ion}}\right)^2} \\ & \times \ln\left(\frac{5}{4} \beta_{i-\mathrm{ion}} \times \frac{E}{E_{i-\mathrm{ion}}}\right), \end{aligned} \tag{5}$$

where ξ_i is the number of energetically equivalent electrons in shell i, $\alpha_{i-\mathrm{ion}}$ and $\beta_{i-\mathrm{ion}}$ are level-dependent parameters.[19,20]

The Einstein radiative transition probabilities of argon could be obtained in the NIST database[34] or by theoretical calculations. For the 4s−4p and 4s−5p transitions, the data recommended by Wiese *et al.*[35] are used while all the other data come from Lilly,[36] Katsonis and Drawin.[37] Since the model contains lumped levels, the effective transition probabilities from and towards effective energy levels are calculated from values of each individual levels by weighting their degeneracies.[37]

To describe the radiation trapping effect, an 'effective' transition probability was introduced. The Einstein transition probability should be multiplied by an 'escape factor' Λ,[19]

$$A^{\mathrm{eff}}_{ji} = \Lambda_{ji} A_{ji}, \tag{6}$$

where j and i are higher and lower levels, Λ_{ji} is the relevant escape factor. For most radiations the low pressure plasma is 'optically thin' and therefore we could neglect the self-absorption, taking $\Lambda = 1$. When it comes to the resonance radiation ($i = 1$), however, there will be serious self-absorption making the transparent plasma approximation invalid and the escape factor should be taken into account, calculated by the Holstein formula.[20,38] Besides the resonance radiation, it is found that the radiation trapping effect may also be important for transitions ending on metastable states and thus we calculate escape factors for these transitions.[39,40]

Besides the above mentioned collisional and radiative processes, an additional diffusion loss term is

important for the two metastable states ($j = 2$, 4) and should also be taken into account. The equation proposed by Chantry[41] and the diffusion coefficient given by Tachibana[42] are used. Processes like three-body recombination and photoionisation are neglected here. The three-body recombination process is not important in discharges with $T_e \geq 1$ eV and $n_e \leq 10^{13}$ cm^{-3}.[1] Neglecting these minor processes could simplify the model without losing accuracies.

For a given excited state j ($j \geq 2$) its population and depopulation processes will be balanced when the discharge is in steady state

$$\sum_{\substack{i=1\\ i\neq j}}^{22} k_{ij}(T_e) n_e n_i + \sum_{i>j} A_{ij}^{\text{eff}} n_i - \sum_{\substack{i=1\\ i\neq j}}^{22} k_{ji}(T_e) n_e n_j - k_{j-\text{ion}}(T_e) n_e n_j - \sum_{i<j} A_{ji}^{\text{eff}} n_j - k_{j,\text{diffu loss}} n_j = 0. \quad (7)$$

The two positive terms denote electron impact and radiative gain from other states while the four negative terms denote electron impact, ionisation, radiative and diffusion loss processes for state j. The last diffusion loss term is only important for the two metastable states ($j = 2$, 4). For convenience, Eq. (7) could be rewritten as

$$\sum_{\substack{i=1\\ i\neq j}}^{22} k_{ij}(T_e) n_e \eta_i + \sum_{i>j} A_{ij}^{\text{eff}} \eta_i - \sum_{\substack{i=1\\ i\neq j}}^{22} k_{ji}(T_e) n_e \eta_j - k_{j-\text{ion}}(T_e) n_e \eta_j - \sum_{i<j} A_{ji}^{\text{eff}} \eta_j - k_{j,\text{diffu loss}} \eta_j = 0, \quad (8)$$

where $\eta_j = n_j/n_g$ is the normalised population density and $n_g = P/(k_B T_g)$, P is the argon gas pressure, k_B is the Boltzmann constant, T_g is the gas temperature in K and in our experiment it was assumed to be 400 K. For the low ionisation degree in our CCP discharge, typically lower than 10^{-3}, we have

$$\sum_{j=1}^{22} \eta_j = 1. \quad (9)$$

There are 24 unknown quantities (22 effective levels densities, i.e., η_1 to η_{22}, and n_e, T_e) in Eqs. (8) and (9). When n_e and T_e are given, it becomes a linear system of equations which could be easily solved. Similarly if two other quantities are given (e.g., the intensities of two spectral lines which are correlated to two levels densities) the equations could also be solved in principle.

3. Experiment

The CCP reactor used in our study was described elsewhere.[43] The inner diameter of the vacuum chamber is 300 mm and diameters of the two parallel plate electrodes, upper and lower, are 220 mm and 200 mm, respectively. The upper water-cooled electrode is powered by the 13.56 MHz frequency power source through an L-type matching box and the lower electrode is grounded. The gap between the two parallel electrodes is kept at 45 mm and a pure argon gas (99.999%) is introduced into the chamber via a mass flow controller. In this experiment, the gas pressure range is controlled from 1 to 5 Pa by a throttle valve.

A Langmuir probe (Hiden ESPion) is used to measure the electron density and the electron temperature. The probe tip is placed at the centre of the chamber when probe is used to acquire the I–V characteristic during the plasma on period. An optical emission spectrometer (AvaSpec-2048FT-8-RM) was used to measure intensities of the emission lines with different wavelengths in the discharge. The wavelength resolution of the spectrometer is 0.05–0.13 nm and the wavelength range is 200–900 nm. Both the probe and OES fibre are fixed at the same plane 2.5 cm below the upper electrode plane.

4. Results and discussion

Since small energy difference with other radiative states and their relative high densities, the metastables could be important for the population of radiative states. Figure 1 shows the contour plot of the first metastable state (level 2, $4s[3/2]_2$) as a function of electron density and electron temperature at 2 Pa pressure. The contour plot of the other metastable state (level 4, $4s'[1/2]_0$) is similar. It could be seen from Fig. 1(a) that the metastable density shows a weak dependence on electron density n_e as n_e is lower than 10^{10} cm^{-3}. From Eq. (8) we have

$$\eta_2 = \frac{n_e \left(k_{1,2}(T_e)\eta_1 + \sum_{i=3}^{22} k_{i,2}(T_e)\eta_i \right) + \sum_{i>2} A_{i,2}^{\text{eff}} \eta_i}{n_e \left(\sum_{\substack{i=1\\ i\neq 2}}^{22} k_{2,i}(T_e) + k_{2-\text{ion}}(T_e) \right) + k_{2,\text{diffu loss}}}.$$

(10)

When the diffusion coefficient in denominator is neglected and if we suppose that η_2 is mainly populated by electron impact from the ground state ($\eta_1 \approx 1$), then it is obvious that η_2 will be independent of the electron density n_e. However, diffusion is an important loss term for the two metastables especially at low pressures. The contour plot in Fig. 1(b) shows significant difference with that in Fig. 1(a). For example, for the condition of $n_e = 10^{10}$ cm^{-3} and $T_e = 3$ eV, η_2 is about 5.0×10^{-4} when we neglect the diffusion loss while it decreases to 3.0×10^{-4} when the diffusion loss term is considered. This result indicates that the loss due to diffusion may be comparable to the electron impact loss processes and it can not be neglected for the two metastable states under our experimental conditions.

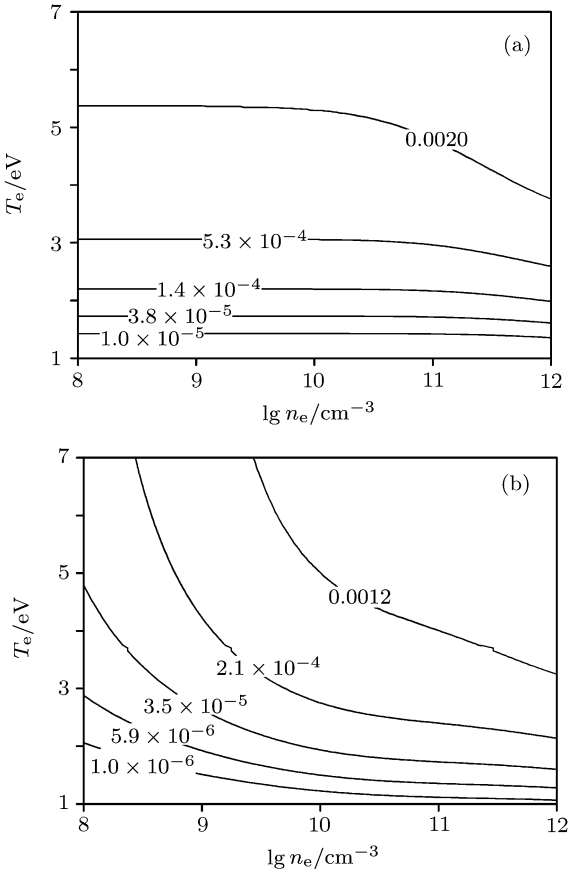


Fig. 1. Population density variation of level 2 with electron density and temperature under 2 Pa pressure: (a) neglecting the diffusion loss; (b) considering the diffusion loss.

In Fig. 2 we present the contour plot of the first radiative state (level 3, $4s[3/2]_1$) as a function of n_e and T_e under 2 Pa pressure. It is obvious that the trend of η_3 is different from η_2 and η_3 has typically smaller orders of magnitude. Take level 3 as an example of the radiative states we could rewrite Eq. (8) as

$$\eta_3 = \frac{n_e\left(k_{1,3}(T_e)\eta_1 + \sum\limits_{\substack{i=2\\ i\neq3}}^{22} k_{i,3}(T_e)\eta_i\right) + \sum\limits_{i>3} A_{i,3}^{\text{eff}}\eta_i}{n_e\left(\sum\limits_{\substack{i=1\\ i\neq3}}^{22} k_{3,i}(T_e) + k_{3-\text{ion}}(T_e)\right) + A_{3,1}^{\text{eff}}}. \tag{11}$$

Since the typical radiative coefficient is in the order of 10^6 s^{-1}, much larger than the electron impact loss term in low pressure CCP discharges, we could neglect the electron impact loss processes in the denominator. If we still suppose that η_3 is mainly populated by electron impact excitation from the ground state (the case in corona model) then η_3 will be proportional to electron density n_e. However, η_3 does not increase linearly with n_e strictly, this reflects that electron impact excitation and radiative decay from other excited states are also important gain processes for level 3. Take $n_e = 5 \times 10^9$ cm^{-3} and $T_e = 3$ eV (typical for low pressure CCP discharges) at 2 Pa pressure as an example, when diffusion loss term of metastable states is neglected, η_3 increases more than 50%. At the same time, η_{10} and η_{11}, population densities of level 10 and 11 ($4p'[1/2]_1$, $4p'[1/2]_0$) which are responsible for several emission lines with strong intensities, increase by about 40% and 3%, respectively.

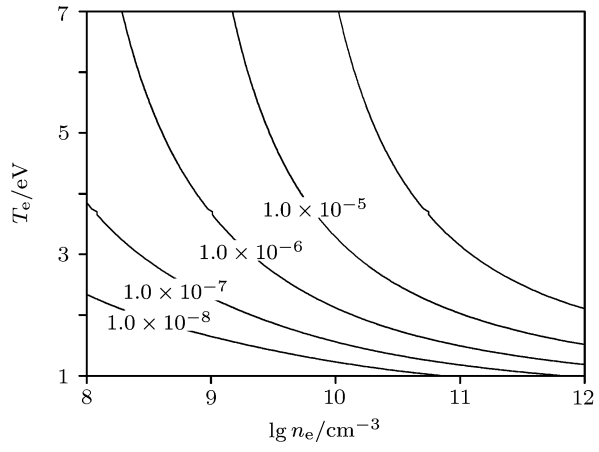


Fig. 2. Population density variation of level 3 with electron density and temperature under 2 Pa pressure.

The contour plot of level 10 ($4p'[1/2]_1$, which is responsible for the radiation with emission line wavelength of 696.5 nm) is shown in Fig. 3(a). It can be seen that the behaviour of this radiative state is similar to that of level 3, i.e., increases with increasing

electron density and temperature. However, its density is orders of magnitude lower than level 3 under the same electron density and electron temperature. This is natural due to its higher excitation energy. Behaviour of level 11 ($4p'[1/2]_0$, the upper level of the strong emission with wavelength of 750.4 nm) is similar to level 10 and is presented in Fig. 3(b).

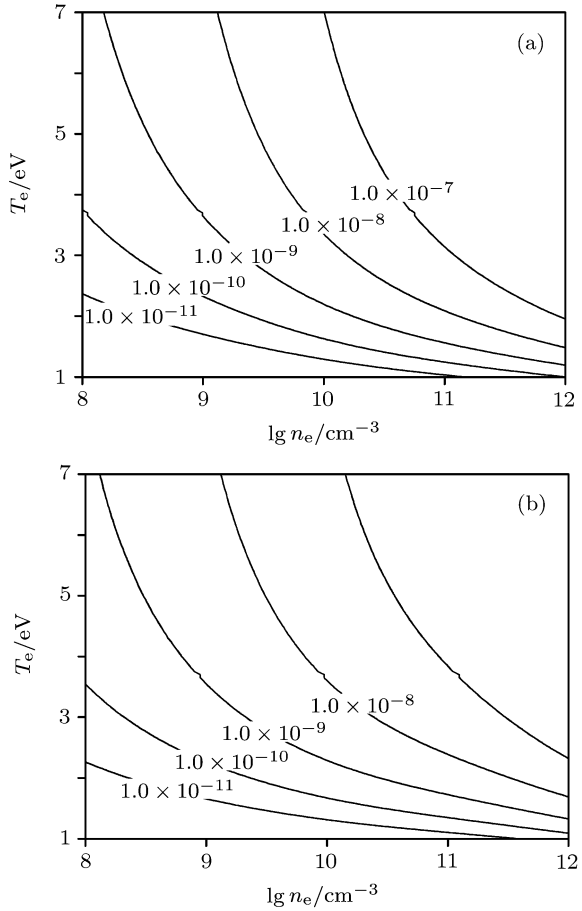


Fig. 3. Population density variation of level 10 (a) and level 11 (b) with electron density and temperature under 2 Pa pressure.

To measure the electron density and temperature two strong emission lines with wavelengths 750.4 nm ($4p'[1/2]_0 \rightarrow 4s'[1/2]_1$) and 696.5 nm ($4p'[1/2]_1 \rightarrow 4s[3/2]_2$) are selected. The procedure to obtain n_e and T_e is similar to that proposed by Palmero *et al.*[17] As has been mentioned, the escape factors of these two emission lines are calculated.[39,40,44] The Ar emission intensity is calibrated with n_e and T_e measured by Langmuir probe at RF power of 200 W and pressure of 2 Pa. In Figs. 4 and 5 electron density n_e and electron temperature T_e taken from OES with CR model are presented, along with measurement results from Langmuir probe. As the input power increases from 100 W to 300 W, n_e increases while T_e decreases at 2 Pa pressure. When the power is maintained at 200 W, n_e increases and T_e decreases with the pressure increasing from 1 to 5 Pa. It can be seen that the results from both methods agree well with each other. A little deviation for these data occurs, which may be due to gas temperature variation with changing measurement conditions. In our group, we have measured the nitrogen (N_2) rotational temperature in N_2 CCP, and observed the gas temperature change with power and gas pressure.[43] A similar behaviour of Ar gas temperature is also expected.

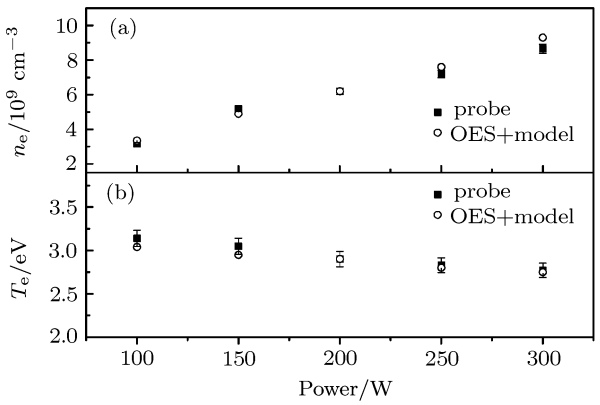


Fig. 4. Results of electron density (a) and temperature (b) as a function of RF power obtained from the model and Langmuir probe at 2 Pa pressure.

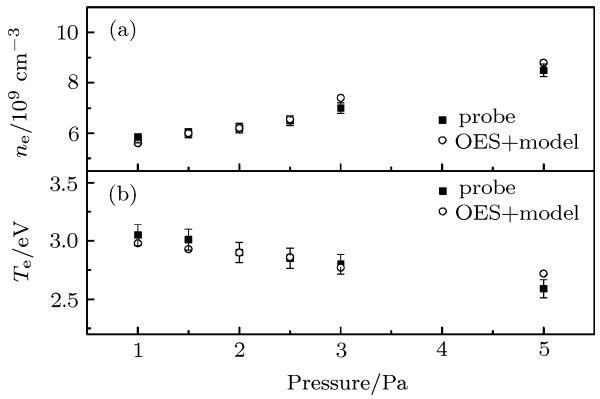


Fig. 5. Results of electron density (a) and temperature (b) as a function of gas pressure obtained from the model and Langmuir probe at 200 W power.

5. Conclusion

We have presented a simplified CR model applicable to capacitively coupled Ar plasma driven at 13.56 MHz. The main processes considered in the model are electron impact excitation, radiative decay and diffusion loss. The role of each process in the balance equations of the excited states is also discussed.

Electron impact and diffusion loss are the main loss processes for the two metastable states while for the other excited states the spontaneous radiative decay processes dominate. In the determination of electron density and temperature, escape factors of the relevant emissions are taken into account. Electron density and temperature obtained from our model agree well with that from Langmuir probe, indicating that the current CR model in combination with OES could be used in diagnosis of RF CCP.

References

[1] Lieberman M A and Lichtenberg A J 2005 *Principles of Plasma Discharges and Materials Processing* (2nd ed.) (Hoboken, NJ: Wiley) pp1, 14, 299

[2] Huang S, Xin Y and Ning Z Y 2005 *Chin. Phys.* **14** 1608

[3] Xu X, Li L S, Liu F, Zhou Q H and Liang R Q 2008 *Chin. Phys.* B **17** 4242

[4] Nagai M and Horia M 2006 *J. Vac. Sci. Technol.* A **24** 1760

[5] Yuan Y, Ye C, Huang H W, Shi G F and Ning Z Y 2010 *Chin. Phys.* B **19** 065205

[6] Goto H H, Lowe H D and Ohmi T 1992 *J. Vac. Sci. Technol.* A **10** 3048

[7] Boyle P C, Ellingboe A R and Turner M M 2004 *J. Phys.* D: *Appl. Phys.* **37** 697

[8] Colgan M J, Meyyappan M and Murnick D E 1994 *Plasma Sources Sci. Technol.* **3** 181

[9] Zhu X M, Chen W C, Zhang S, Guo Z G, Hu D W and Pu Y K 2007 *J. Phys.* D: *Appl. Phys.* **40** 7019

[10] Chen F F 1965 in: Huddlestone R H and Leonard S L (eds.) *Plasma Diagnostic Techniques* (New York: Academic) p113

[11] Sudit I D and Chen F F 1994 *Plasma Sources Sci. Technol.* **3** 162

[12] Ahn S K, You S J and Chang H Y 2006 *Appl. Phys. Lett.* **89** 161506

[13] Ahn S K and Chang H Y 2009 *Appl. Phys. Lett.* **95** 111502

[14] Donnelly V M 2004 *J. Phys.* D: *Appl. Phys.* **37** R217

[15] Malyshev M V and Donnelly V M 1999 *Phys. Rev.* E **60** 6016

[16] Stafford L, Khare R, Donnelly V M, Margot J and Moisan M 2009 *Appl. Phys. Lett.* **94** 021503

[17] Palmero A, van Hattum E D, Rudolph H and Habraken F H P M 2007 *J. Appl. Phys.* **101** 053306

[18] Zhu X M and Pu Y K 2007 *J. Phys.* D: *Appl. Phys.* **40** 2533

[19] Vlcek J 1989 *J. Phys.* D **22** 623

[20] Bogaerts A, Gijbels R and Vlcek J 1998 *J. Appl. Phys.* **84** 121

[21] Bultel A, van Ootegem B, Bourdon A and Vervisch P 2002 *Phys. Rev.* E **65** 046406

[22] Iordanova S and Koleva I 2007 *Spectrochim. Acta* B **62** 344

[23] Yanguas-Gil A, Cotrino J and Gonzalez-Elipe A R 2005 *Phys Rev.* E **72** 016401

[24] Yanguas-Gil A, Cotrino J and Gonzalez-Elipe A R 2006 *J. Appl. Phys.* **99** 033104

[25] Akatsuka H 2009 *Phys. Plasmas* **16** 043502

[26] Boffard J B, Lin C C and DeJoseph Jr C A 2004 *J. Phys.* D: *Appl. Phys.* **37** R143

[27] Chutjian A and Cartwright D C 1981 *Phys. Rev.* A **23** 2178

[28] Bretagne J, Godart J and Puech V 1982 *J. Phys.* D **15** 2205

[29] Hyman H A 1978 *Phys. Rev.* A **18** 441

[30] Kimura A, Kobayashi H, Nishida M and Valentin P 1985 *J. Quant. Spectrosc. Radiat. Transfer* **34** 189

[31] Chilton J E, Boffard J B, Schappe R S and Lin C C 1998 *Phys. Rev.* A **57** 267

[32] Boffard J B, Piech G A, Gehrke M F, Anderson L W and Lin C C 1999 *Phys. Rev.* A **59** 2749

[33] Yanguas-Gil A, Cotrino J and Alves L L 2005 *J. Phys.* D: *Appl. Phys.* **38** 1588

[34] NIST 2009 *Atomic Spectra Database*

[35] Wiese W L, Brault J W, Danzmann K, Helbig V and Kock M 1989 *Phys. Rev.* A **39** 2461

[36] Lilly R A 1976 *J. Opt. Soc. Am.* **66** 245

[37] Katsonis K and Drawin H W 1980 *J. Quant. Spectrosc. Radiat. Transfer* **23** 1

[38] Holstein T 1951 *Phys. Rev.* **83** 1159

[39] Zhu X M and Pu Y K 2010 *J. Phys.* D: *Appl. Phys.* **43** 015204

[40] Boivin R F, Kline J L and Scime E E 2001 *Phys. Plasmas* **8** 5303

[41] Chantry P J 1987 *J. Appl. Phys.* **62** 1141

[42] Tachibana K 1986 *Phys. Rev.* A **34** 1007

[43] Huang X J, Xin Y, Yuan Q H and Ning Z Y 2008 *Phys. Plasmas* **15** 073501

[44] McWhirter R W P 1965 in: Huddlestone R H and Leonard S L (eds.) *Plasma Diagnostic Techniques* (New York: Academic) p201